Pricing Vulnerable Spread Options under an Intensity-based Model*

Hongwei Bi, Xingchun Wang, Nanyi Zhang†

Abstract

This paper proposes an intensity-based model to price spread options with default risk. In our framework, default risk is captured by a Cox process, whose intensity is correlated with the volatility (two underlying assets). In addition, a general correlation between the intensity and the volatility (two underlying assets) is allowed. We obtain an analytical expression of approximated prices of vulnerable spread options using the probability measure-change method. Finally, numerical results are performed to demonstrate the accuracy of the approximation and illustrate the effect of default risk.

Keywords: Vulnerable Spread Options; Intensity-based Model; Default Risk; Cox Process.

JEL classification: G13

1 Introduction

Spread options refer to a type of options whose payoff is based on the difference between the prices of two underlying assets. The underlying assets can be stocks or bonds, and the payoff of a spread call option with maturity T and strike price K can be written as $(S_1(T) - S_2(T) - K)^+$, where $S_1(T)$ and $S_2(T)$ are the prices of the underlying assets.

Several models have been applied to price spread options. One approach is to directly model the spread, or the difference between two underlying assets, called univariate modeling (see, e.g., Dempster [7]). However, the univariate model ignores the correlation between the underlying assets, which is essential for pricing spread options. The other approach concentrates on the dynamics of the underlying assets, known as explicit modeling. For example, Margrabe [17] assumed that the underlying assets follow two-factor Geometric Brownian Motions (2GBM) and derived the pricing formula of spread options with zero strike price. In

*Hongwei Bi and Nanyi Zhang are at the School of Insurance and Economics, University of International Business and Economics, Beijing 100029, China. Xingchun Wang is at the School of International Trade and Economics, University of International Business and Economics, Beijing 100029, China.

†Corresponding author. Email: 201930035@uibe.edu.cn

addition, copula methods are also used to capture the correlation structure (see, e.g., Cherubini and Luciano [4]). The literature on spread options focus on analytic approximations since there is no explicit pricing formula for the spread option when $K \neq 0$. Kirk and Bajita [14] initiated a well-known approximation formula of spread option prices with non-zero strike price. Carmona and Durrleman[3] put forward an analytic estimation with different bound families. Numerical experiments suggested that their approximations are very close for some parameter values. Deelstra [6] developed an approximation formula based on the moment matching method and harmonic theory. Bjerksund and Stensland [2] proposed a lower bound that is more precise in numerical experiments compared with Kirk's approximation. However, these literature did not consider the counterparty risk associated with spread options.

oOptions with default risk, known as vulnerable options, have been widely investigated in the previous literature. Johnson and Stulz [11] first used the structural model to incorporate default risk and assumed that default occurs when the option's value is larger than the writer's assets at option maturity. Klein [15] extended the model in Johnson and Stulz [11] to a more general setting. In addition, Alos et al. [1] considered vulnerable European options with default risk in a stochastic volatility model. Wang and Zhou [19] decompose the stochastic volatility into long-term and short-term volatility and use a mean-reverting process to describe the short-term volatility, while the long-term volatility is considered to remain constant. Apart from structural models, intensity-based models have also received much attention (see, e.g., Cherubini and Luciano [5] and Lando [16]). This framework directly models the default time rather than modeling the writer's assets. Especially, Wang [20] investigated European and Asian options with default risk in which the Cox process is applied to describe the default time.

In this paper, we propose an intensity-based model to value vulnerable spread options. In particular, we assume that the dynamics of the two underlying assets follow a three-factor stochastic volatility (SV) process, and the default risk is captured by a Cox process. We suppose a more general correlation between the intensity and the volatility (two underlying assets) better fits the real world. In the proposed pricing model, the intensity and the two underlying asset prices can be correlated positively or negatively. Moreover, with a particular parameter value ($\beta_2 = 0$), the intensity process in this paper has the same form as that in Wang [20], and hence the pricing model in this paper includes the one in Wang [20] as a particular case. We obtain the analytical expressions of approximated prices of vulnerable spread options by establishing an approximate exercise region and using the probability measure change method. The derived pricing formulae generalize the previous literature; that is, many existing pricing formulae can be obtained from the derived pricing formulae by simply changing some parameters. Finally, the approximation proposed under the three-factor SV model is highly accurate, as shown in the numerical examples.

The paper is structured as follows. In Section 2, the theoretical framework is described, and the approximate pricing formula is derived. Section 3 presents the numerical results. Section 4 concludes.

2 Model description and pricing

In this section, vulnerable spread options are priced in an intensity-based model. To this end, we employ a three-factor stochastic volatility model to describe the dynamics of the two underlying assets, and use a Cox process to capture default risk. To price the options with default risk, we also need to expand the filtration to include the default time τ. More specifically, set

$$\mathcal{F}_t = \mathcal{G}_t \vee \mathcal{H}_t, \text{ and } \mathcal{H}_t = \sigma\{I_{(\tau \leqslant s)}, 0 \leqslant s \leqslant t\},$$

where $\mathcal{G}_t$ is generated by the asset prices, the volatility, and the intensity process. In addition, we suppose that the discounted asset prices are martingales with respect to this expanded filtration $\mathcal{F}_t$ under risk-neutral probability measure Q. With the above assumption, we introduce the pricing model and derive the analytical expression of vulnerable spread options with default risk using the probability measure-change method.

2.1 The Model

In this subsection, we introduce the pricing model. Let us start with the dynamics of the two underlying assets. Following Dempster and Hong [8], we assume the following three-factor stochastic volatility model (under risk-neutral probability measure),

$$\begin{cases} \frac{\mathrm{d}S_1(t)}{S_1(t)} = r\mathrm{d}t + \sigma_1\sqrt{V(t)}\mathrm{d}B_1(t), \\ \frac{\mathrm{d}S_2(t)}{S_2(t)} = r\mathrm{d}t + \sigma_2\sqrt{V(t)}\mathrm{d}B_2(t), \\ \mathrm{d}V(t) = (\gamma_0 - \alpha_0 V(t))\mathrm{d}t + \sigma_V\sqrt{V(t)}\mathrm{d}B_3(t), \end{cases}$$

where r is the risk-free interest rate, $\sqrt{V(t)}$ multiplied by σ_1 or σ_2 denotes the volatility of the underlying assets, and B_1, B_2, B_3 are standard Brownian motions with the following correlation structure,

$$\begin{aligned} \langle B_1, B_2\rangle_t &= \rho t, \\ \langle B_1, B_3\rangle_t &= \rho_1 t, \\ \langle B_1, B_2\rangle_t &= \rho_2 t. \end{aligned}$$

When $\gamma_0 = \alpha_0 = \sigma_V = 0$, $V(t)$ reduces to a constant $V(0)$, and the model becomes to be the 2GBM framework (see, e.g., Shimko [18]).

In what follows, we incorporate default risk into the model. The default is treated as an unexpected event, which occurs at time τ, the first jump time of the Cox process. Once a default occurs, only a proportion of a can be recovered. Besides, we suppose that the intensity of the Cox process is driven by

$$\lambda(t) = \beta_1 V(t) + \frac{\beta_2}{V(t)} + Y(t), \tag{2.1}$$

where β_1 and β_2 are non-negative constants, and $Y(t)$ describes the idiosyncratic risk of option issuers. In addition, we assume that the dynamic of $Y(t)$ is given by

$$\mathrm{d}Y(t) = (\gamma_1 - \alpha_1 Y(t))\mathrm{d}t + \sigma_Y \sqrt{Y(t)}\mathrm{d}L(t), \tag{2.2}$$

where $L(t)$ is a standard Brownian motion independent of $B_1(t)$, $B_2(t)$ and $B_3(t)$, since $L(t)$ is used to capture the idiosyncratic risk of option issuers.

Notice that in our framework, the CIR process is applied to describe the default intensity and the volatility. Thus, the parameters should be chosen to guarantee the existence of strong solutions (see, e.g., Karatzas and Shreve [12] and Kim and Wee [13]). It should also be remarked that the two terms $\beta_1 V(t)$ and $\frac{\beta_2}{V(t)}$ in (2.1) capture a general correlation between the default intensity and the underlying asset prices because the default intensity may be positively (e.g., $\beta_2 = 0$) or negatively (e.g., $\beta_1 = 0$) correlated with $V(t)$. Moreover, with $\beta_2 = 0$, the above intensity process has the same form as that in Wang [20], and hence the pricing model in this paper extends the one in Wang [20] to a more general case in essence.

2.2 The Characteristic Function

To obtain the pricing formulae, here we derive the joint characteristic function of $\ln S_1(T)$, $\ln S_2(T)$, $\int_0^T \lambda(s)\mathrm{d}s$. More precisely, take

$$f(\phi_1, \phi_2, \phi_3) := \mathbb{E}[\mathrm{e}^{\phi_1 \ln S_1(T) + \phi_2 \ln S_2(T) + \phi_3 \int_0^T \lambda(s)\mathrm{d}s}], \ \ \phi_1, \phi_2, \phi_3 \in \mathbb{C}, \tag{2.3}$$

where $\mathbb{C} = \{x + iy : (x, y) \in \mathbb{R}^2\}$. We present the result in the following proposition.

Proposition 2.1. *(The joint characteristic function) For any ϕ_1, ϕ_2, $\phi_3 \in \mathbb{C}$, we have that*

$$\begin{aligned} f(\phi_1, \phi_2, \phi_3) = {} & \mathrm{e}^{\phi_1\left[\ln S_1(0) + rT - \frac{\sigma_1\rho_1}{\sigma_V}(V(0) + \gamma_0 T)\right] + \phi_2\left[\ln S_2(0) + rT - \frac{\sigma_2\rho_2}{\sigma_V}(V(0) + \gamma_0 T)\right]} \times G_Y(\phi_3, 0, 0) \\ & \times G_V\Bigg(\phi_1\Big(\frac{\sigma_1\rho_1\alpha_0}{\sigma_V} - \frac{1}{2}\sigma_1^2\Big) + \phi_2\Big(\frac{\sigma_2\rho_2\alpha_0}{\sigma_V} - \frac{1}{2}\sigma_2^2\Big) + \frac{1}{2}\phi_1^2\sigma_1^2(1 - \rho_1^2) + \frac{1}{2}\phi_2^2\sigma_2^2(1 - \rho_2^2) \\ & + \phi_1\phi_2\sigma_1\sigma_2(\rho - \rho_1\rho_2) + \phi_3\beta_1, \ \ \phi_1\frac{\sigma_1\rho_1}{\sigma_V} + \phi_2\frac{\sigma_2\rho_2}{\sigma_V}, \phi_3\beta_2\Bigg), \end{aligned} \tag{2.4}$$

where $G_V(z_1, z_2, z_3) = \mathbb{E}\left[\mathrm{e}^{z_1\int_0^T V(s)\mathrm{d}s + z_2 V(T) + z_3\int_0^T \frac{\mathrm{d}s}{V(s)}}\right]$ and $G_Y(z_1, z_2, z_3) = \mathbb{E}\left[\mathrm{e}^{z_1\int_0^T Y(s)\mathrm{d}s + z_2 Y(T) + z_3\int_0^T \frac{\mathrm{d}s}{Y(s)}}\right]$. Specially, the expression of $G_V(\cdot,\cdot,\cdot)$ and $G_Y(\cdot,\cdot,\cdot)$ can be explicitly derived as Grasselli [9].

Proof. Step 1. *Decompose $B_1(t)$ and $B_2(t)$.*

We write $B_1(t)$ and $B_2(t)$ in the following form,

$$\begin{cases} \mathrm{d}B_1(t) = \rho_1\mathrm{d}B_3(t) + \sqrt{1 - \rho_1^2}\mathrm{d}\tilde{B}_1(t), \\ \mathrm{d}B_2(t) = \rho_2\mathrm{d}B_3(t) + \sqrt{1 - \rho_2^2}\mathrm{d}\tilde{B}_2(t), \end{cases} \tag{2.5}$$

where $\tilde{B}_k(t)$ $(k=1,2)$ are standard Brownian motions independent of $B_3(t)$ and $\mathrm{d}\langle\tilde{B}_1(t),\tilde{B}_2(t)\rangle = \frac{\rho-\rho_1\rho_2}{\sqrt{1-\rho_1^2}\sqrt{1-\rho_2^2}}\mathrm{d}t$ with $-1 < \frac{\rho-\rho_1\rho_2}{\sqrt{1-\rho_1^2}\sqrt{1-\rho_2^2}} < 1$. For the volatility process, we have that

$$\int_0^T \sqrt{V(t)}\ \mathrm{d}B_3(t) = \frac{1}{\sigma_V}\left(V(T) - V(0) - \gamma_0 T + \alpha_0 \int_0^T V(t)\mathrm{d}t\right).$$

Then $\ln S_1(T)$ can be written as

$$\begin{aligned}
\ln S_1(T) &= \ln S_1(0) + rT + \int_0^T \sigma_1\sqrt{V(s)}\mathrm{d}B_1(s) - \frac{1}{2}\int_0^T \sigma_1^2 V(s)\mathrm{d}s \\
&= \ln S_1(0) + rT - \frac{\sigma_1\rho_1}{\sigma_V}(V(0)+\gamma_0 T) + \frac{\sigma_1\rho_1}{\sigma_V}V(T) + (\frac{\sigma_1\rho_1\alpha_0}{\sigma_V} - \frac{1}{2}\sigma_1^2)\int_0^T V(s)\mathrm{d}s \\
&\quad + \int_0^T \sqrt{1-\rho_1^2}\sigma_1\sqrt{V(s)}\mathrm{d}\tilde{B}_1(t).
\end{aligned}$$

Notice that this is also true for $\ln S_2(T)$.

Step 2. *Separating the linear combination into independent parts.*

We deduce from Step 1 that,

$$\begin{aligned}
&\phi_1 \ln S_1(T) + \phi_2 \ln S_2(T) + \phi_3 \int_0^T \lambda(s)\mathrm{d}s \\
&= \phi_1\left[\ln S_1(0) + rT - \frac{\sigma_1\rho_1}{\sigma_V}(V(0)+\gamma_0 T)\right] + \phi_2\left[\ln S_2(0) + rT - \frac{\sigma_2\rho_2}{\sigma_V}(V(0)+\gamma_0 T)\right] \\
&+ \left[\phi_1\left(\frac{\sigma_1\rho_1\alpha_0}{\sigma_V} - \frac{1}{2}\sigma_1^2\right) + \phi_2\left(\frac{\sigma_2\rho_2\alpha_0}{\sigma_V} - \frac{1}{2}\sigma_2^2\right) + \phi_3\beta_1\right]\int_0^T V(s)\mathrm{d}s \\
&+ \left(\phi_1\frac{\sigma_1\rho_1}{\sigma_V} + \phi_2\frac{\sigma_2\rho_2}{\sigma_V}\right)V(T) + \phi_3\beta_2\int_0^T \frac{1}{V(s)}\mathrm{d}s \\
&+ \phi_1\sqrt{1-\rho_1^2}\sigma_1\int_0^T \sqrt{V(s)}\mathrm{d}\tilde{B}_1(s) + \phi_2\sqrt{1-\rho_2^2}\sigma_2\int_0^T \sqrt{V(s)}\mathrm{d}\tilde{B}_2(s) \\
&+ \phi_3\int_0^T Y(s)\mathrm{d}s.
\end{aligned}$$

For simplicity in presentation, we define ν, ν_0, ν_1, ν_2 as follows,

$$\begin{cases}
\nu(\phi_1,\phi_2) = \phi_1\left[\ln S_1(0) + rT - \frac{\sigma_1\rho_1}{\sigma_V}(V(0)+\gamma_0 T)\right] + \phi_2\left[\ln S_2(0) + rT - \frac{\sigma_2\rho_2}{\sigma_V}(V(0)+\gamma_0 T)\right], & \text{(2.6a)} \\
\nu_1(\phi_1,\phi_2) = \phi_1\sqrt{1-\rho_1^2}\sigma_1\int_0^T \sqrt{V(s)}\mathrm{d}\tilde{B}_1(s) + \phi_2\sqrt{1-\rho_2^2}\sigma_2\int_0^T \sqrt{V(s)}\mathrm{d}\tilde{B}_2(s), & \text{(2.6b)} \\
\nu_2(\phi_3) = \phi_3\int_0^T Y(s)\mathrm{d}s, & \text{(2.6c)} \\
\nu_0(\phi_1,\phi_2,\phi_3) = \left[\phi_1\left(\frac{\sigma_1\rho_1\alpha_0}{\sigma_V} - \frac{1}{2}\sigma_1^2\right) + \phi_2\left(\frac{\sigma_2\rho_2\alpha_0}{\sigma_V} - \frac{1}{2}\sigma_2^2\right) + \phi_3\beta_1\right]\int_0^T V(s)\mathrm{d}s + \\
\qquad \left(\phi_1\frac{\sigma_1\rho_1}{\sigma_V} + \phi_2\frac{\sigma_2\rho_2}{\sigma_V}\right)V(T) + \phi_3\beta_2\int_0^T \frac{1}{V(s)}\mathrm{d}s. & \text{(2.6d)}
\end{cases}$$

By definition, $\nu(\phi_1,\phi_2)$ is a constant; $\nu_2(\phi_3)$ is only affected by $L(t)$ that makes it independent of $\nu_0(\phi_1,\phi_2,\phi_3)$ and $\nu_1(\phi_1,\phi_2)$. In addition, $\nu_0(\phi_1,\phi_2,\phi_3)$ is $\sigma(B_3(t))_{\{0\leqslant t\leqslant T\}}$-measurable since $V(t)$ is driven by $B_3(t)$.

Step 3. *Integrating*

An application of the law of iterated expectation yields that

$$\begin{aligned}
&\mathbb{E}\left[\mathrm{e}^{\nu_0(\phi_1,\phi_2,\phi_3)+\nu_1(\phi_1,\phi_2)}\right]\\
=\;&\mathbb{E}\left[\mathrm{e}^{\nu_0(\phi_1,\phi_2,\phi_3)}\,\mathbb{E}\left[\mathrm{e}^{\nu_1(\phi_1,\phi_2)}\,\middle|\sigma(B_3(t))_{\{0\leqslant t\leqslant T\}}\right]\right]\\
=\;&\mathbb{E}\left[\mathrm{e}^{\nu_0(\phi_1,\phi_2,\phi_3)+\frac{1}{2}\left[\left(\phi_1^2\sigma_1^2(1-\rho_1^2)+\phi_2^2\sigma_2^2(1-\rho_2^2)+2\phi_1\phi_2\sigma_1\sigma_2(\rho-\rho_1\rho_2)\right)\int_0^T V(s)\mathrm{d}s\right]}\right]\\
=\;&\mathbb{E}\Bigg[\exp\Bigg\{\Big[\phi_1(\frac{\sigma_1\rho_1\alpha_0}{\sigma_V}-\frac{1}{2}\sigma_1^2)+\phi_2(\frac{\sigma_2\rho_2\alpha_0}{\sigma_V}-\frac{1}{2}\sigma_2^2)+\frac{1}{2}\phi_1^2\sigma_1^2(1-\rho_1^2)+\frac{1}{2}\phi_2^2\sigma_2^2(1-\rho_2^2)\\
&\quad+\phi_1\phi_2\sigma_1\sigma_2(\rho-\rho_1\rho_2)+\phi_3\beta_1\Big]\int_0^T V(s)\mathrm{d}s+(\phi_1\frac{\sigma_1\rho_1}{\sigma_V}+\phi_2\frac{\sigma_2\rho_2}{\sigma_V})V(T)+\phi_3\beta_2\int_0^T\frac{1}{V(s)}\mathrm{d}s\Bigg\}\Bigg]\\
=\;&G_V\Bigg(\phi_1(\frac{\sigma_1\rho_1\alpha_0}{\sigma_V}-\frac{1}{2}\sigma_1^2)+\phi_2(\frac{\sigma_2\rho_2\alpha_0}{\sigma_V}-\frac{1}{2}\sigma_2^2)+\frac{1}{2}\phi_1^2\sigma_1^2(1-\rho_1^2)+\frac{1}{2}\phi_2^2\sigma_2^2(1-\rho_2^2)\\
&\quad+\phi_1\phi_2\sigma_1\sigma_2(\rho-\rho_1\rho_2)+\phi_3\beta_1,\;\phi_1\frac{\sigma_1\rho_1}{\sigma_V}+\phi_2\frac{\sigma_2\rho_2}{\sigma_V},\phi_3\beta_2\Bigg).
\end{aligned}$$

Finally, together with the fact that $\mathbb{E}[\mathrm{e}^{\nu_2(\phi_3)}]=\mathbb{E}[\mathrm{e}^{\phi_3\int_0^T Y(s)\mathrm{d}s}]$ equals $G_Y(\phi_3,0,0)$, we obtain (2.4). □

2.3 The Pricing Formulae

In this subsection, we introduce a procedure for evaluating the value of vulnerable spread options. Recall that T is the expiration time, and K is the strike price of the option. According to the risk-neutral pricing theory, the price of spread options with default risk has the following form,

$$\begin{aligned}
VSO\;=\;&\mathrm{e}^{-rT}\,\mathbb{E}\Big[I(\tau>T)(S_1(T)-S_2(T)-K)^+\Big]\\
&+\mathbb{E}\Big[I(0<\tau\leq T)a\,\mathrm{e}^{-r\tau}\,\mathbb{E}\Big[\mathrm{e}^{-r(T-\tau)}(S_1(T)-S_2(T)-K)^+|\mathcal{F}_\tau\Big]\Big] \qquad (2.7)\\
=\;&\mathrm{e}^{-rT}\,\mathbb{E}\Big[I(\tau>T)(S_1(T)-S_2(T)-K)^+\Big]+a\,\mathrm{e}^{-rT}\,\mathbb{E}\Big[I(0<\tau\leq T)(S_1(T)-S_2(T)-K)^+\Big],
\end{aligned}$$

where τ is the first jump time, and a is the recovery rate. The closed-form expression for the variable VSO can be derived via the inverse Fourier transforms of the expression $(e^{x_1}+e^{x_2}-1)^+$, as detailed in Hurd and Zhou [10]. Nevertheless, given the intricate nature of the quadratic integration involved, an approximation of the exercise boundary is employed for simplification.

To be specific, we first consider the following event A,

$$A=\left\{\omega:\frac{S_1(T)}{S_2^\alpha(T)}>\frac{\mathrm{e}^k}{E[S_2^\alpha(T)]}\right\}, \qquad (2.8)$$

where α and k are chosen to ensure that A is close to the exercise region. Event A was first proposed in Bjerksund and Stensland [2], where they chose

$$\alpha=\frac{S_2(0)\mathrm{e}^{rT}}{S_2(0)\mathrm{e}^{rT}+K},\quad k=\ln(S_2(0)\mathrm{e}^{rT}+K), \qquad (2.9)$$

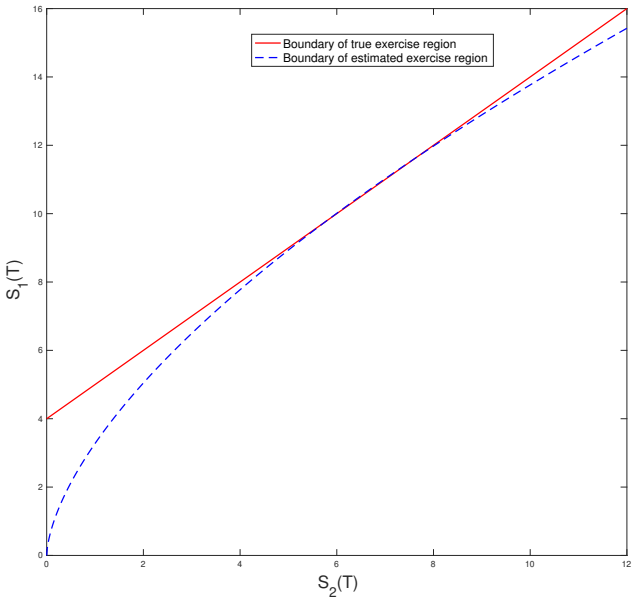

Figure 1: True exercise boundary v.s. Estimated exercise boundary.

and checked that the approximation is highly accurate under some circumstances. The essence of the above approximation is to approximate the line $(S_2(T)+K)$ using a power function $(\frac{\mathrm{e}^k}{E[S_2^\alpha(T)]}S_2^\alpha(T))$. To further explain the idea of our approximation, we plot these curves in Figure 1, where the area above the red line represents the true exercise area and the area above the blue curve represents the estimated exercise area. Since the joint density is mainly concentrated around the point $(\mathrm{E}(S_1(T)),\ \mathrm{E}(S_2(T)))$, thus this approximation is reasonable and expected to be highly close to the fair value.

The power function degenerates to the line when the strike price equals zero. We define the following event (exercise region)

$$B = \{\omega : S_1(T) \geqslant S_2(T) + K\}\,.$$

If $K = 0$, then we have $\alpha = 1$ and $\mathrm{e}^k = E[S_2(T)]$, so $A = B$. This means the approximation gives the fair value of exchange options.

Now we consider the following approximation,

$$(S_1(T) - S_2(T) - K)^+ \approx (S_1(T) - S_2(T) - K)\, I_A. \tag{2.10}$$

Substituting 2.10 into 2.7, we have the following approximated vulnerable spread option price,

$$ASO = (1-a)\,\mathrm{e}^{-rT}\,\mathbb{E}\Big[I(\tau > T)(S_1(T) - S_2(T) - K)I_A\Big] + a\,\mathrm{e}^{-rT}\,\mathbb{E}\Big[(S_1(T) - S_2(T) - K)I_A\Big]. \tag{2.11}$$

We can further rewrite ASO as follows,

$$ASO = (1-a)\,\mathrm{e}^{-rT}\left(AS_1 - AS_2 - K * AS_3\right) + a\,\mathrm{e}^{-rt}\left(AS_4 - AS_5 - K * AS_6\right), \tag{2.12}$$

where AS_1-AS_6 are given by

$$AS_1 = \mathbb{E}\left[\mathrm{e}^{\ln S_1(T)}\, I_{\{\tau>T,\ A\}}\right], \quad AS_2 = \mathbb{E}\left[\mathrm{e}^{\ln S_2(T)}\, I_{\{\tau>T,\ A\}}\right], \quad AS_3 = \mathbb{E}\left[I_{\{\tau>T,\ A\}}\right],$$
$$AS_4 = \mathbb{E}\left[\mathrm{e}^{\ln S_1(T)}\, I_A\right], \qquad AS_5 = \mathbb{E}\left[\mathrm{e}^{\ln S_2(T)}\, I_A\right], \qquad AS_6 = \mathbb{E}\left[I_A\right].$$

The mathematical expressions of AS_1-AS_6 are derived in the following proposition.

Proposition 2.2. *(The expression of AS_1-AS_6) Note that $D = \ln\frac{\mathrm{e}^k}{E\left[S_2^{\alpha}(T)\right]}$, then we have that*

$$\begin{aligned}
AS_1 &= \frac{1}{2}f(1,0,-1) + \frac{1}{\pi}\int_0^{+\infty} Re\left[\frac{\mathrm{e}^{-itD}\, f(it+1,-iat,-1)}{it}\right]\mathrm{d}t,\\
AS_2 &= \frac{1}{2}f(0,1,-1) + \frac{1}{\pi}\int_0^{+\infty} Re\left[\frac{\mathrm{e}^{-itD}\, f(it,-iat+1,-1)}{it}\right]\mathrm{d}t,\\
AS_3 &= \frac{1}{2}f(0,0,-1) + \frac{1}{\pi}\int_0^{+\infty} Re\left[\frac{\mathrm{e}^{-itD}\, f(it,-iat,-1)}{it}\right]\mathrm{d}t,\\
AS_4 &= \frac{1}{2}f(1,0,0) + \frac{1}{\pi}\int_0^{+\infty} Re\left[\frac{\mathrm{e}^{-itD}\, f(it+1,-iat,0)}{it}\right]\mathrm{d}t,\\
AS_5 &= \frac{1}{2}f(0,1,0) + \frac{1}{\pi}\int_0^{+\infty} Re\left[\frac{\mathrm{e}^{-itD}\, f(it,-iat+1,0)}{it}\right]\mathrm{d}t,\\
AS_6 &= \frac{1}{2}f(0,0,0) + \frac{1}{\pi}\int_0^{+\infty} Re\left[\frac{\mathrm{e}^{-itD}\, f(it,-iat,0)}{it}\right]\mathrm{d}t.
\end{aligned}$$

Proof. We first focus on how to calculate AS_1. Notice that a Cox process is a Poisson process with random intensity. In our framework, the process itself is independent of market filtration, but the intensity is not. Thus, AS_1 can be expressed as follows,

$$\begin{aligned}
AS_1 &= \mathbb{E}\left[\mathrm{e}^{\ln S_1(T)}\, I_{\{\tau>T,\ A\}}\right]\\
&= \mathbb{E}\left[\mathrm{e}^{\ln S_1(T)}\, I_A E[I_{\{\tau>T\}}|\mathcal{G}_T]\right]\\
&= \mathbb{E}\left[\mathrm{e}^{\ln S_1(T)-\int_0^T\lambda(s)\mathrm{d}s}\, I_A\right],
\end{aligned}$$

where we have used the fact that τ and I_A are independent under regular probability measure $Q(\cdot|\mathcal{G}_T)(\omega)$ in the second equality. Next, we introduce a new probability measure Q_1,

$$Q_1(A) := \frac{\int_A \mathrm{e}^{\ln S_1(T)-\int_0^T\lambda(s)\mathrm{d}s}\,\mathrm{d}Q(\omega)}{\int_\Omega \mathrm{e}^{\ln S_1(T)-\int_0^T\lambda(s)\mathrm{d}s}\,\mathrm{d}Q(\omega)}.$$

Since $\mathrm{e}^{\ln S_1(T)-\int_0^T\lambda(s)\mathrm{d}s} > 0$, then we have $Q_1 \ll Q$ and $Q \ll Q_1$, and hence the Radon-Nikodym derivative of Q_1 with respect to Q is

$$\frac{\mathrm{d}Q_1}{\mathrm{d}Q} = \frac{\mathrm{e}^{\ln S_1(T)-\int_0^T\lambda(s)\mathrm{d}s}}{\int_\Omega \mathrm{e}^{\ln S_1(T)-\int_0^T\lambda(s)\mathrm{d}s}\,\mathrm{d}Q(\omega)}.$$

Thus the characteristic function of $\ln S_1(T) - a \ln S_2(T)$ under Q_1 is given by

$$\mathbb{E}^{Q_1}\left[\mathrm{e}^{it(\ln S_1(T) - a \ln S_2(T))}\right] = \frac{f(it+1, -iat, -1)}{f(1,0,-1)}.$$

Therefore, one gets that

$$\begin{aligned}
AS_1 &= \mathbb{E}\left[\mathrm{e}^{\ln S_1(T) - \int_0^T \lambda(s)\mathrm{d}s)} I_A\right] \\
&= \mathbb{E}\left[\mathrm{e}^{\ln S_1(T) - \int_0^T \lambda(s)\mathrm{d}s)}\right] \mathbb{E}^{Q_1}\left[I_A\right] \\
&= f(1,0,-1) * Q_1\{\ln S_1(T) - \alpha * \ln S_2(T) > D\} \\
&= f(1,0,-1) * \left(\frac{1}{2} + \frac{1}{\pi}\int_0^{+\infty} Re\left[\frac{\mathrm{e}^{-itD} f(it+1, -iat, -1)/f(1,0,-1)}{it}\right]\mathrm{d}t\right) \\
&= \frac{1}{2} f(1,0,-1) + \frac{1}{\pi}\int_0^{+\infty} Re\left[\frac{\mathrm{e}^{-itD} f(it+1, -iat, -1)}{it}\right]\mathrm{d}t,
\end{aligned}$$

where the fourth equality follows from the relationship between the characteristic function and the survival function(Gil-Pelaez).

Similarly, AS_2 can be calculated by introducing another probability measure Q_2,

$$Q_2(A) := \frac{\int_A \mathrm{e}^{\ln S_2(T) - \int_0^T \lambda(s)\mathrm{d}s}\,\mathrm{d}Q(\omega)}{\int_\Omega \mathrm{e}^{\ln S_2(T) - \int_0^T \lambda(s)\mathrm{d}s}\,\mathrm{d}Q(\omega)}.$$

Therefore, we obtain

$$\begin{aligned}
AS_2 &= \mathbb{E}\left[\mathrm{e}^{\ln S_2(T) - \int_0^T \lambda(s)\mathrm{d}s} I_A\right] \\
&= \mathbb{E}\left[\mathrm{e}^{\ln S_2(T) - \int_0^T \lambda(s)\mathrm{d}s}\right] \mathbb{E}^{Q_2}\left[I_A\right] \\
&= f(0,1,-1) * Q_2\{\ln S_1(T) - \alpha * \ln S_2(T) > D\} \\
&= f(0,1,-1) * \left(\frac{1}{2} + \frac{1}{\pi}\int_0^{+\infty} Re\left[\frac{\mathrm{e}^{-itD} f(it, -iat+1, -1)/f(1,0,-1)}{it}\right]\mathrm{d}t\right) \\
&= \frac{1}{2} f(0,1,-1) + \frac{1}{\pi}\int_0^{+\infty} Re\left[\frac{\mathrm{e}^{-itD} f(it, -iat+1, -1)}{it}\right]\mathrm{d}t.
\end{aligned}$$

The expression of AS_3-AS_6 can also be derived similarly. Thus we choose to omit them. This completes the proof of Proposition 2.2. □

Remark 2.1. *Adding additional assets into the model, our results can be extended to a more general case. Specifically, we can estimate the price of a basket of options under stochastic volatility models. Similar results are given in Wang and Zhang [21] in which they derive an approximation expression of a basket of options with default risk under Heston-Nandi garch models.*

3 Numerical results

In this section, we present numerical examples to show the accuracy of the approximation and analyze the impact of default risk. Because the approximated pricing formula in Proposition 2.2 is in the form of

Table 1: Parameter values

Parameters in the underlying asset dynamics		
Initial value	$S_1(0) = 100$	$S_2(0) = 96$
Volatility coefficient	$\sigma_1 = 1.0$	$\sigma_2 = 0.5$
Parameters in volatility dynamics	$V(0) = 0.04$	$\sigma_V = 0.05$
	$\alpha_0 = 1.0$	$\gamma_0/\alpha_0 = 0.04$
Correlation structure	$\rho_1 = -0.5$	$\rho_2 = 0.25$
	$\rho = 0.5$	
Parameters in the intensity of Cox process		
Initial value	Y(0)=0.037	
Parameters governing default intensities	$\beta_1 = 0.8$	$\beta_2 = 0$
	$\alpha_1 = 2.0$	$\gamma_1/\alpha_1 = 0.01$
	$\sigma_Y = 0.10$	
Other parameters		
Interest rate	$r = 0.05$	
Strike price	$K = 4$	
Maturity	$T = 2.0$	
Recovery rate	$a = 0.40$	

improper integrals, the convergence must be checked.

We use the parameter values in Table 1 and take the upper bound of integral (UL) as 10^1, 10^2, 10^3 and 10^4 respectively, to illustrate the convergence. In addition, Monte Carlo simulations are employed for comparison.[1] Table 2 displays the prices of spread options[2] together with vulnerable spread options with various strike prices and maturities. It can be seen that the integral converges fast, and the numerical results remain constant when the upper bound is larger than 10^2. Therefore, we choose $UL = 10^3$ in the following analysis. We can also find that the approximation is so close to the actual price that it can be seen as a good approximation.

To further check the accuracy of the approximation, we vary other parameters in the pricing framework. In Tables 3 and 4, we vary the values of $\sigma_1, \sigma_2, \beta_1, \beta_2$ respectively, and then compare them with the values generated by Monte Carlo simulations. We can see from the tables that our approximation is still good in all these cases.

In what follows, we illustrate the impact of default risk by changing different parameter values. For comparison, we report vulnerable spread option prices with $\beta_2 = 0$, $\beta_2 = 0.20$ and $\beta_2 = 0.40$ in each figure. Specially, the corresponding default probability $(1 - f(0, 0, -1))$ against time to maturities T is plotted in Figure 2. Figures 3 and 4 illustrate options prices with alternative strike prices and different maturities.

[1] We run 100,000 paths daily to obtain the price. In addition, to avoid negative variance in the volatility and intensity processes, we follow Kim and Wee [13] to use the full truncation scheme. The relevant codes are available on https://github.com/nymath/tree/main/VSP.

[2] The price of vanilla spread options can be obtained by setting $a = 1$ in (2.12).

Intuitively, all option prices decrease as strike prices rise. From Figure 4, we can observe that the difference between spread options and vulnerable spread options widens as maturity increases. This is because the default probability rises with an increase of time to maturities, as shown in Figure 2. The increasing default probability reduces the value of the options significantly. Figure 5 displays how option prices change with the value of β_1 in the intensity process. Notice that the prices of spread options remain the same in this case. In addition, larger β_1 corresponds to a larger intensity, leading to a higher default probability and thus a lower price of vulnerable spread options.

Figures 6 and 7 exhibit options prices against different initial values of $V(0)$ in the volatility process. A sizeable initial value $V(0)$ of the volatility process induces a larger difference in the option values in the short term ($T = 2$). However, in the long term ($T = 5$), as shown in Figure 7, the slope of the price curve is more flat, which means the initial value has much less influence on the price in the long term. Note that the level of volatility has two distinct effects. On the one hand, it increases the uncertainty of future prices, enhancing the value of the options. On the other hand, it affects the intensity process, as defined in (2.1). The default intensity rises as the level of volatility increases, reducing vulnerable spread option prices. Figures 6 and 7 show that the channel through future prices plays a dominant role. The effects of the long-term levels of volatility are shown in Figures 8 and 9, indicating that long-term levels of volatility have more significant effects on the options with longer maturity.

Figures 10 and 11 plot spread option prices in the proposed model when the values of ρ_1 and ρ_2 vary. A similar trend occurs for the price of spread options and vulnerable spread options as $(\rho_1,\ \rho_2)$ approaches $(1,\ 1)$ or $(-1,\ -1)$; while an opposite trend occurs when $(\rho_1,\ \rho_2)$ approaches $(1,\ -1)$ or $(-1,\ 1)$. It can be seen that a higher value of ρ_1 or ρ_2 indicates that an increment of $B_3(t)$ is more likely to induce the significant values of $B_1(t)$ and $B_2(t)$. This increases the volatility of $S_1(t)$ and $S_2(t)$, and hence the spread options prices rise.

4 Conclusion

In this paper, an intensity-based model is used to price vulnerable spread options. In the proposed framework, the dynamics of the two underlying assets are driven by a three-factor stochastic volatility model and the default risk is captured by a Cox process. In addition, we assume a general correlation between the default intensity and the volatility (underlying assets). Since there is no explicit formula for the price of spread options with non-zero strikes, we derive an approximation by establishing an approximate exercise region and using the probability measure-change method. Numerical analysis is conducted to demonstrate the accuracy and sensitivity of the approximation.

Table 2: Prices of the options calculated using the approximation formula in Proposition 2.2 and the values generated by MC. In addition, U stands for the upper limit of the improper integrals, and the numbers in brackets are the standard deviations of the simulations.

			Spread Options			Vulnerable Spread Options		
T	K	U	Price	CPU	Monte Carlo	Price	CPU	Monte Carlo
0.5	4	10^1	3.8436	0.37	4.9314[0.0237]	3.7794	0.16	4.8484[0.0233]
		10^2	4.9232	0.20		4.8403	0.25	
		10^3	4.9232	0.21		4.8403	0.18	
		10^4	4.9232	0.35		4.8403	0.49	
	8	10^1	2.2151	0.24	3.2582[0.0195]	2.1784	0.15	3.2036[0.0192]
		10^2	3.2602	0.23		3.2055	0.17	
		10^3	3.2602	0.77		3.2055	0.16	
		10^4	3.2602	0.68		3.2055	0.25	
	12	10^1	1.1509	0.11	2.0559[0.0155]	1.1319	0.11	2.0207[0.0153]
		10^2	2.0534	0.18		2.0191	0.18	
		10^3	2.0534	0.24		2.0191	0.15	
		10^4	2.0534	0.28		2.0191	0.21	
1.5	4	10^1	8.2640	0.18	8.5734[0.0431]	7.9215	0.43	8.2176[0.0414]
		10^2	8.5534	0.12		8.1982	0.10	
		10^3	8.5534	0.20		8.1982	0.18	
		10^4	8.5534	0.25		8.1982	0.21	
	8	10^1	6.6067	0.12	6.8967[0.0392]	6.3336	0.10	6.6114[0.0376]
		10^2	6.9152	0.15		6.6290	0.09	
		10^3	6.9152	0.18		6.6290	0.38	
		10^4	6.9152	0.47		6.6290	0.51	
	12	10^1	5.2368	0.25	5.5244[0.0354]	5.0208	0.26	5.2966[0.0339]
		10^2	5.5262	0.24		5.2983	0.20	
		10^3	5.5262	0.36		5.2983	0.25	
		10^4	5.5262	0.41		5.2983	0.46	
3.0	4	10^1	12.0968	0.23	12.1704[0.0647]	11.2055	0.19	11.3303[0.0606]
		10^2	12.1224	0.30		11.2289	0.17	
		10^3	12.1224	0.47		11.2289	0.43	
		10^4	12.1224	0.44		11.2289	0.25	
	8	10^1	10.5806	0.1	10.6625[0.0616]	9.8028	0.10	9.8791[0.0571]
		10^2	10.6161	0.13		9.8354	0.17	
		10^3	10.6161	0.24		9.8354	0.44	
		10^4	10.6161	0.62		9.8354	0.47	
	12	10^1	9.2234	0.13	9.2607[0.0576]	8.5468	0.11	8.5811[0.0534]
		10^2	9.2645	0.11		8.5848	0.11	
		10^3	9.2645	0.23		8.5848	0.23	
		10^4	9.2645	0.25		8.5848	0.24	

Table 3: Approximations of spread options and fair values generated by simulations with different values of volatilities. (sd stands for the sample standard deviation of Monte Carlo simulations)

	Vulnerable Spread Options				Vulnerable Spread Options		
σ_1	Price	Monte Carlo	sd	σ_2	Price	Monte Carlo	sd
0	5.3060	5.3106	0.0220	0	10.7560	10.7253	0.0566
0.1	4.8689	4.8263	0.0198	0.1	10.2921	10.2825	0.0544
0.2	4.6465	4.6965	0.0191	0.2	9.9115	9.9104	0.0526
0.3	4.6708	4.6733	0.0194	0.3	9.6246	9.5938	0.0506
0.4	4.9381	4.9402	0.0211	0.4	9.4407	9.3290	0.0489
0.5	5.4108	5.4303	0.0240	0.5	9.3661	9.3119	0.0479
0.6	6.0388	6.0582	0.0277	0.6	9.4038	9.4371	0.0479
0.7	6.7772	6.7968	0.0322	0.7	9.5524	9.5804	0.0476
0.8	7.5923	7.5720	0.0369	0.8	9.8069	9.8020	0.0477
0.9	8.4605	8.5118	0.0425	0.9	10.1589	10.1489	0.0485
1	9.3661	9.3583	0.0483	1	10.5984	10.5522	0.0492

Table 4: Approximations of spread options and fair values generated by simulations with different values of parameters in the intensity process.

	Vulnerable Spread Options				Vulnerable Spread Options		
β_1	Price	Monte Carlo	sd	β_2	Price	Monte Carlo	sd
0.5	9.4859	9.4698	0.0486	0.002	8.7920	8.7293	0.0452
0.7	9.4058	9.3124	0.0481	0.004	8.2793	8.2616	0.0425
0.9	9.3268	9.3933	0.0483	0.006	7.8214	7.7930	0.0400
1.1	9.2489	9.1923	0.0476	0.008	7.4125	7.3641	0.0378
1.3	9.1722	9.1427	0.0473	0.010	7.0472	7.0368	0.0361
1.5	9.0966	9.0546	0.0468	0.012	6.7208	6.6848	0.0342
1.7	9.0221	9.0076	0.0466	0.014	6.4291	6.3706	0.0325
1.9	8.9487	8.9296	0.0462	0.016	6.1685	6.1838	0.0315

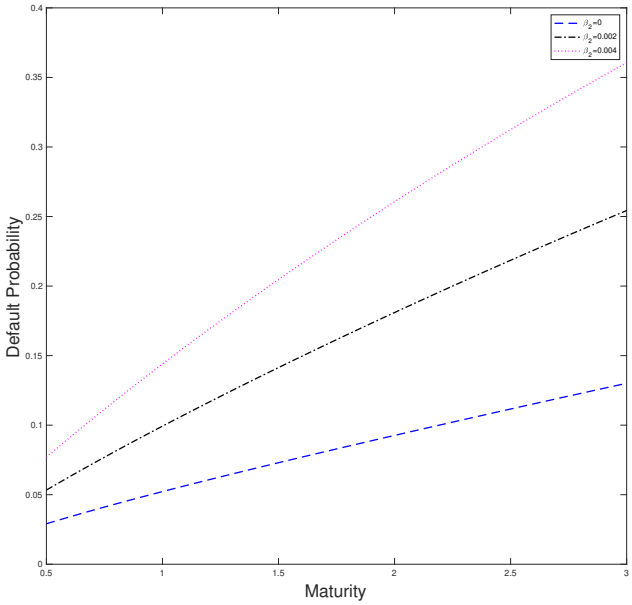

Figure 2: Default probability against time to maturities T.

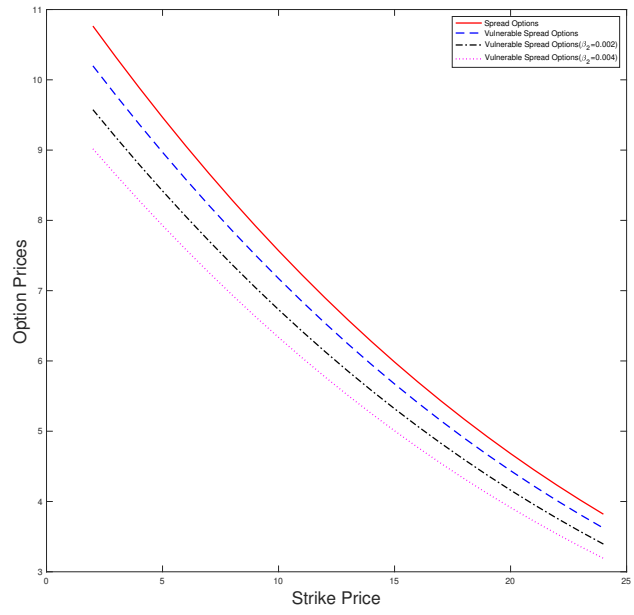

Figure 3: Option prices against strike prices K.

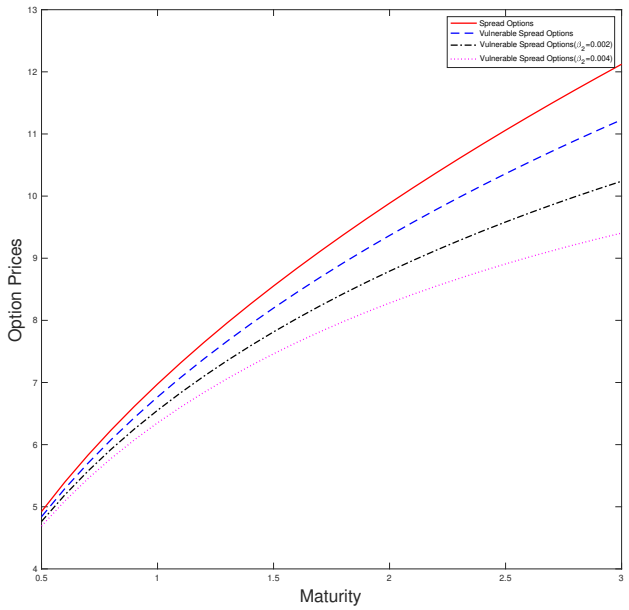

Figure 4: Prices against time to maturities T.

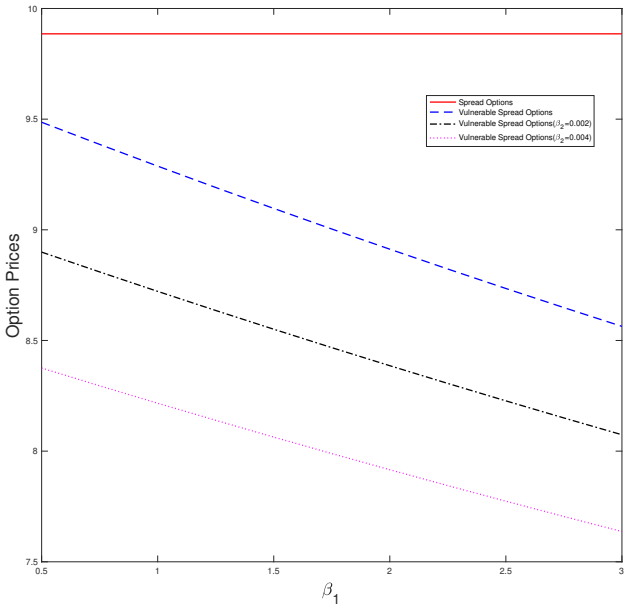

Figure 5: Prices against β_1 in the intensity process.

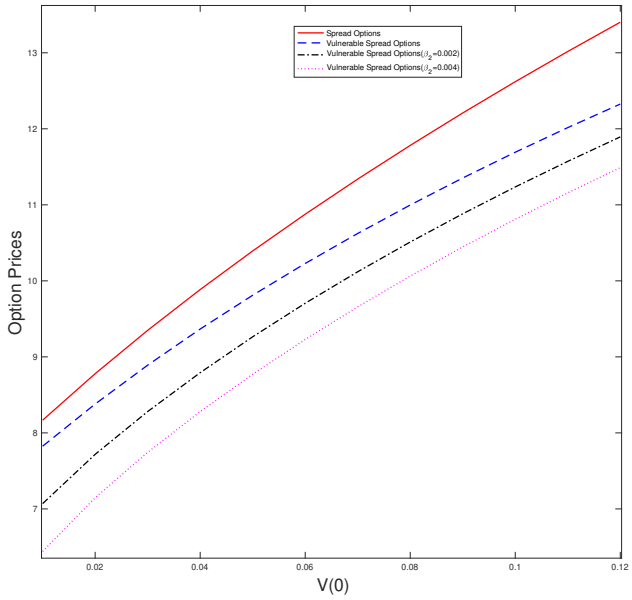

Figure 6: Prices against the initial values $V(0)$ in volatility process.

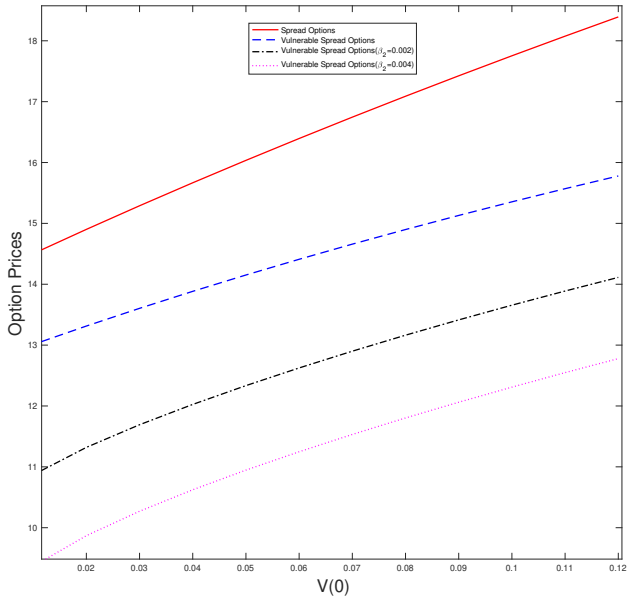

Figure 7: Prices against the initial values $V(0)$ in volatility process with $T = 5$.

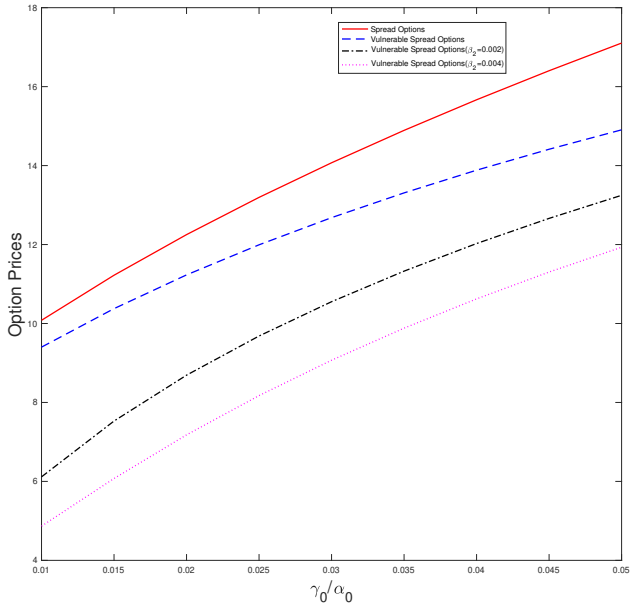

Figure 8: Prices against the long-term volatility of $V(t)$.

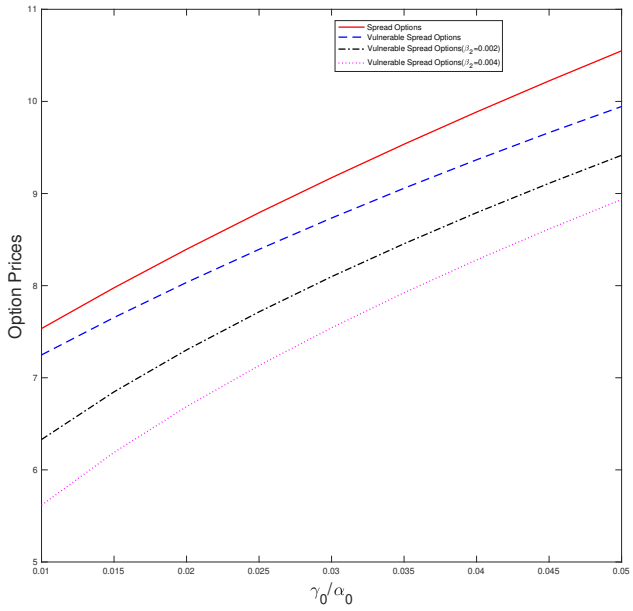

Figure 9: Prices against the long-term volatility of $V(t)$ with $T = 5$.

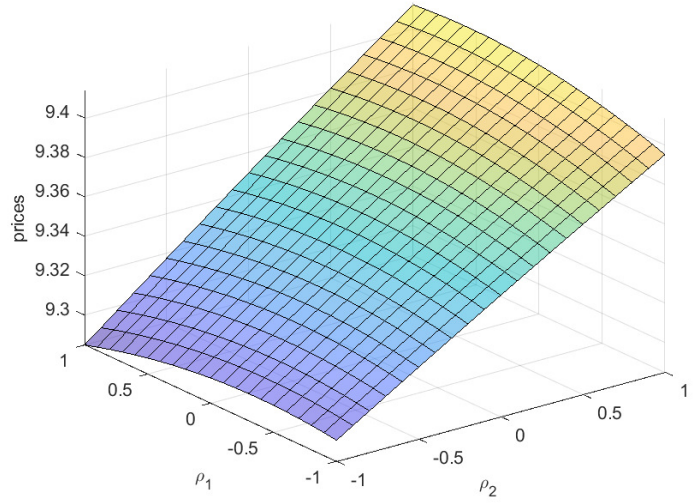

Figure 10: Prices of vulnerable spread option against correlation structure with $\rho = 0.5$.

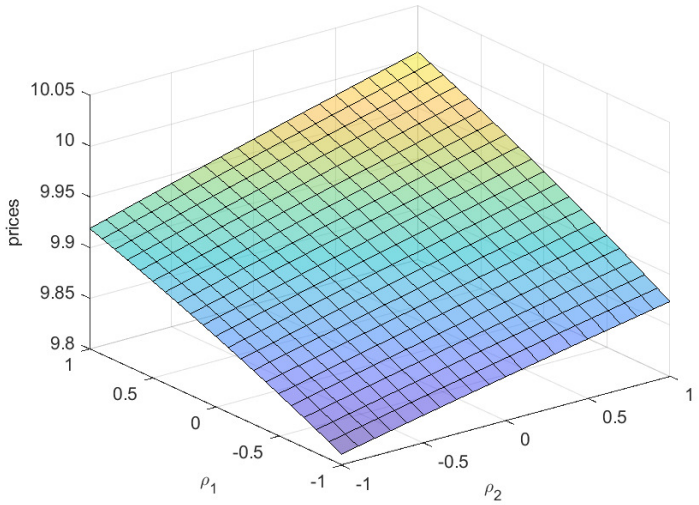

Figure 11: Prices of spread option against correlation structure with $\rho = 0.5$.

References

[1] E. Alos, F. Antonelli, A. Ramponi, and S. Scarlatti. CVA and vulnerable options in stochastic volatility models. *International Journal of Theoretical and Applied Finance*, 24(2):1–34, 2021.

[2] P. Bjerksund and G. Stensland. Closed form spread option valuation. *Quantitative Finance*, 14:1785–1794, 2014.

[3] R. Carmona and V. Durrleman. Pricing and hedging spread options. *Siam Review*, 45:627–685, 2003.

[4] U. Cherubini and E. Luciano. Bivariate option pricing with copulas. *Applied Mathematical Finance*, 9(2):69–85, 2002.

[5] U. Cherubini and E. Luciano. Pricing vulnerable options with copulas. *The Journal of Risk Finance*, 5(1):27–39, 2003.

[6] G. Deelstra, I. Diallo, and M. Vanmaele. Moment matching approximation of asian basket option prices. *Journal of computational and applied mathematics*, 234:1006–1016, 2010.

[7] A. P. Dempster. Upper and lower probabilities induced by a multivalued mapping. In *Classic works of the Dempster-Shafer theory of belief functions*, pages 57–72. Springer, 2008.

[8] M. A. H. Dempster and S. G. Hong. Spread option valuation and the fast fourier transform. In *Mathematical Finance—Bachelier Congress 2000*, pages 203–220. Springer, 2002.

[9] M. Grasselli. The 4/2 stochastic volatility model: A unified approach for the heston and the 3/2 model. *Mathematical Finance*, 27(4):1013–1034, 2017.

[10] T. R. Hurd and Z. Zhou. A fourier transform method for spread option pricing. *SIAM Journal on Financial Mathematics*, 1(1):142–157, 2010.

[11] H. Johnson and R. Stulz. The pricing of options with default risk. *The Journal of Finance*, 42:267–280, 1987.

[12] I. Karatzas, J. P. Lehoczky, S. P. Sethi, and S. E. Shreve. Explicit solution of a general consumption/investment problem. In *Optimal Consumption and Investment with Bankruptcy*, pages 21–56. Springer, 1997.

[13] B. Kim and I.-S. Wee. Pricing of geometric asian options under heston's stochastic volatility model. *Quantitative Finance*, 14:1795–1809, 2014.

[14] G. Kirk and J. Bajita. Root-induced iron oxidation, ph changes and zinc solubilization in the rhizosphere of lowland rice. *New Phytologist*, 131:129–137, 1995.

[15] P. Klein. Pricing black-scholes options with correlated credit risk. *Journal of Banking & Finance*, 20:1211–1229, 1996.

[16] D. Lando. Modelling bonds and derivatives with default risk. *Mathematics of Derivative Securities*, 15:369–393, 1997.

[17] W. Margrabe. The value of an option to exchange one asset for another. *The Journal of Finance*, 33:177–186, 1978.

[18] D. C. Shimko. Options on futures spreads: Hedging, speculation, and valuation. *The Journal of Futures Markets*, 14(2):183–213, 1994.

[19] G. Wang, X. Wang, and K. Zhou. Pricing vulnerable options with stochastic volatility. *Physica A: Statistical Mechanics and its Applications*, 485:91–103, 2017.

[20] X. Wang. Analytical valuation of vulnerable european and asian options in intensity-based models. *Journal of Computational and Applied Mathematics*, 393:113412, 2021.

[21] X. Wang and H. Zhang. Pricing basket spread options with default risk under heston–nandi garch models. *The North American Journal of Economics and Finance*, 59:101596, 2022.